Available online at www.sciencedirect.com
ScienceDirect
Ceramics International 34 (2008) 219–223
CERAMICS INTERNATIONAL
www.elsevier.com/locate/ceramint

Preparation and properties of yttrium-doped $SrTiO_3$ anode materials

Xiu-Fu Sun, Rui-Song Guo *, Juan Li

Key Laboratory of Advanced Ceramics and Machining Technology of Ministry of Education, Tianjin University, Tianjin 300072, China

Received 29 November 2005; received in revised form 22 July 2006; accepted 8 September 2006
Available online 13 November 2006

Abstract

Direct electrochemical oxidation of hydrocarbon fuels is a current development trend of solid oxide fuel cells (SOFCs) and finding new anode materials for this application is a key issue. In this study, promising candidates, Y_2O_3-doped $SrTiO_3$ perovskite compounds $Sr_{1-1.5x}Y_xTiO_3$ ($x = 0.02, 0.04, 0.06, 0.08, 0.10$), were synthesized by solid-state reaction. The structure of the calcined powders was examined by X-ray diffraction (XRD). The sinterability and high temperature conductivity were measured by the Archimedes principle and a dc four-probe method, respectively. The effect of sintering temperature on the electrical conductivity was studied. The results indicated that the optimal sintering temperature is around 1400 °C. From 400 °C to 1000 °C, the conductivity decreased with increasing temperature. At 800 °C the highest conductivity (26.8 S/cm) was observed for $x = 0.08$.

Keywords: A. Powders: solid state reaction; C. Electrical conductivity; D. Perovskites; E. Fuel cell; Anode

1. Introduction

The development of solid oxide fuel cells (SOFCs) became a key issue because of the emergent energy and environment problems. Hydrogen and reforming natural gas were used as fuels for SOFCs for many years. However, wide application of hydrogen as a fuel for SOFCs has been restricted due to the high cost of mass supply and the potential danger. Although the use of internal reforming natural gas can solve these problems, it will make the system more complicated and decrease the fuel efficiency. Furthermore, the carbon deposition is usually unavoidable. The use of Ni/YSZ as an anode may cause grain aggregation of Ni and low sulfur resistance [1–4]. Under these circumstances, the use of hydrocarbons as fuels through direct electrochemical oxidation without carbon deposition could be a very promising alternative. The direct electrochemical oxidation technology will make it possible to use several fuels that are abundant and cheap, including petrol, dimethylmethane, natural gas and so on. It will definitely accelerate the commercialization of SOFCs [5,6]. The anode plays a very important role in catalyzing the hydrocarbon fuels conversion to hydrogen and carbon dioxide. Hence, finding new anode materials that can directly catalyze the hydrocarbon fuels without carbon deposition is critical.

The anode materials for direct catalyzing the hydrocarbons must possess the following characteristics: (1) sufficient electronic conductivity; (2) long-term durability in operating circumstances, no destructive phase transition, matching of the thermal expansion and no chemical reaction with electrolytes; (3) sufficient porosity to allow the fuel gas and byproduct delivery and good catalytic performance without carbon deposition.

Doped $SrTiO_3$ materials possess mixed conductivity and the electrochemical reactions occur over the entire electrode/gas interface. The triple phase contact of electrode, electrolyte and gas is replaced by a simple two-phase boundary region between electrode and gas, thus increasing the electrochemical reaction interface. Furthermore, with a mixed conducting electrode, the polarization losses are expected to be significantly less than for purely electronic conductivity. Also, sulfur poisoning might not be so problematic because ceramics have a lower affinity to sulfur. Studies have showed that doped-$SrTiO_3$ provides excellent electrochemical oxidation of hydrocarbon fuels being considered to be one of the most promising candidates for an SOFC anode [7–10]. In this study, $SrTiO_3$ materials doped with different contents of Y_2O_3 were synthesized. The sintering behavior was determined and the electrical performance was characterized.

* Corresponding author. Current address: School of Materials Science and Engineering, Tianjin University, Tianjin 300072, China.
Fax: +86 22 2740 4724.
E-mail address: rsguo@tju.edu.cn (R.-S. Guo).

0272-8842/$32.00
doi:10.1016/j.ceramint.2006.09.009

2. Experimental procedures

$Sr_{1-1.5x}Y_xTiO_3$ powders ($x = 0.02$, 0.04, 0.06, 0.08, 0.10) were prepared by solid-state reaction and were marked as YST2, YST4, YST6, YST8, and YST10, respectively. $SrCO_3$ (99.9%, Tianjin Kewei Company, China), TiO_2 (99.58%, Xiantao Zhongxing Electrondata Co. Ltd., Hubei Province, China) and Y_2O_3 (99.99%, Shanghai Yuelong Co. Ltd., China) were used as starting materials. The raw materials were mixed by ball milling for 6 h. Then, the mixture was dried and sieved, followed by calcination at 1100 °C for 2 h to obtain solid solutions. The calcination process was determined based on a DSC–TG analysis by NETZCH STA 449C with a heating rate of 5 °C/min until 1300 °C. Bars were shaped by dry pressing at 100 MPa, followed by isostatic compaction at 200 MPa. Bars were sealed in a crucible together with graphite, which created a reducing atmosphere inside the crucible. Samples were sintered for 2 h at 1400 °C and 1450 °C, respectively. The sintering processes were determined by a dilatometer analysis (NETZCH DIL 420C) with the heating rate of 5 °C/min until 1450 °C. After cooling down to room temperature, the density of samples was measured by the Archimedes method and the electrical conductivity was measured with a dc four-probe method from 400 °C to 1000 °C in dry H_2 atmosphere. The conductivity was recorded every 100 °C after soaking for 15 min. A constant dc current source was used to supply the required current and the voltage drop across the probes was measured with one digital multimeter. X-ray diffraction (XRD) was carried out to confirm the phase formation of samples by Philips X-ray diffractometer (Rigaku D/Max 2500/PC), using Cu Kα radiation and Ni filter. The morphology of the sintered samples was observed by environmental scanning electron microscope (PHILIPS XL-30 ESEM).

3. Results and discussion

3.1. DSC–TG analysis

The DSC–TG curves of sample YST8 are shown in Fig. 1. A sharp endothermic peak appeared at 947.3 °C, corresponding to the decomposition of $SrCO_3$ to SrO and CO_2: $SrCO_3 \rightarrow SrO + CO_2$, accompanied by carbon dioxide gas release and weight loss. This process lasts until 1020 °C. Afterwards, a broad exothermic peak appeared at 1100 °C. SrO was highly reactive and reacted with TiO_2 to form $SrTiO_3$; meanwhile, Y_2O_3 dissolved into the solid solution. The reaction during this process in a wide range of temperature can be written as [11]: $(1 - 1.5x)SrO + TiO_2 + 0.5xY_2O_3 \rightarrow Sr_{1-1.5x}V''_{0.5x}Y_xTiO_3$. Therefore, it was determined to soak at 940 °C for 30 min and to end at 1100 °C for 2 h for the calcination process in order to ensure high sinterability of the powders.

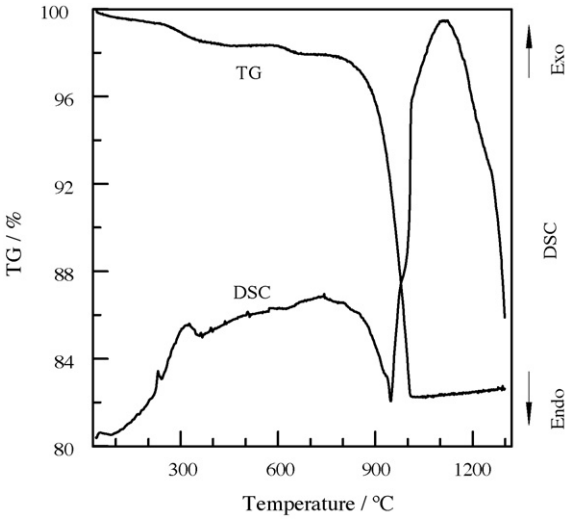

Fig. 1. DSC–TG curves of sample YST8.

3.2. XRD analysis

Fig. 2 shows XRD patterns for the YST8 sample. It can be seen that the formation of $SrTiO_3$ and the dissolution of Y_2O_3 into $SrTiO_3$ were completed after calcination at 1100 °C for 2 h and the powder had a stable perovskite structure compared with the standard pattern of $SrTiO_3$. Based on the XRD data, the crystalline lattice parameter a was calculated as 0.39048 nm and 0.39050 nm for the Y-doped $SrTiO_3$ and pure $SrTiO_3$, respectively, by the following equation:

$$d = \frac{a}{\sqrt{h^2 + k^2 + l^2}}$$

where d is the interplanar distance; a the lattice parameter; h, k and l are the Miller indexes. The theoretical densities of samples with different amounts of dopant can be derived based on the formula of solid solutions. The results are listed in Table 1.

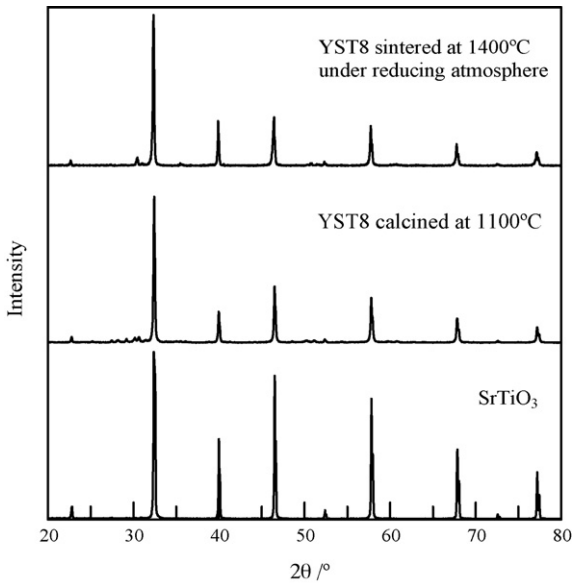

Fig. 2. XRD patterns of sample YST8 calcined at 1100 °C for 2 h and sintered at 1400 °C for 2 h.

Table 1
Theoretical density of samples with different Y_2O_3 content

Samples	Theoretical density (g cm^{-3})
YST2	5.05
YST4	5.03
YST6	5.01
YST8	4.98
YST10	4.96

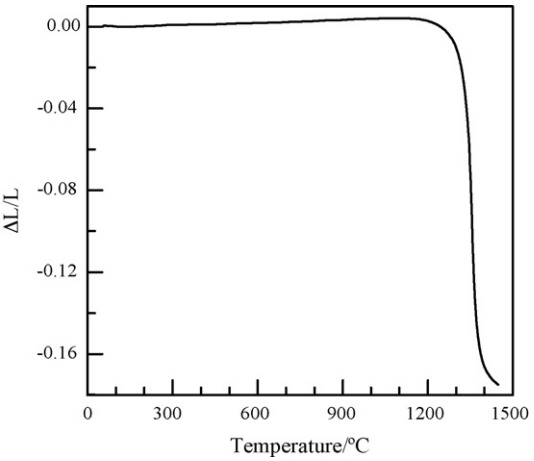

Fig. 3. Dilatometer analysis of sample YST8.

3.3. Sintering

The relation between shrinkage and temperature, which was determined by a dilatometer is shown in Fig. 3. At first, the sample expanded with increasing temperature up to 1200 °C because of the thermal expansion, and then shrank abruptly. A lower shrinkage rate was observed from 1370 °C to 1400 °C, revealing that the sintering process came to the final stage. Therefore, two sintering temperatures of 1400 °C and 1450 °C were chosen to identify the density of sintered samples. The relative density of samples doped with different Y_2O_3 contents are shown in Fig. 4. It can be seen that relative densities continuously decreased with increasing Y_2O_3 content. This is because the grain size of doped-$SrTiO_3$ is highly sensitive to the dopant content [12,13]. At low donor concentrations, grain growth may become pronounced during high temperature sintering; but at high doping concentrations, grain growth is suppressed, which caused more pores and defects and resulted in lower density. However, the relative density larger than 92% was still obtained for all samples. XRD (see Fig. 2) indicated that SYT8 still had a single perovskite structure after sintering in reducing atmosphere.

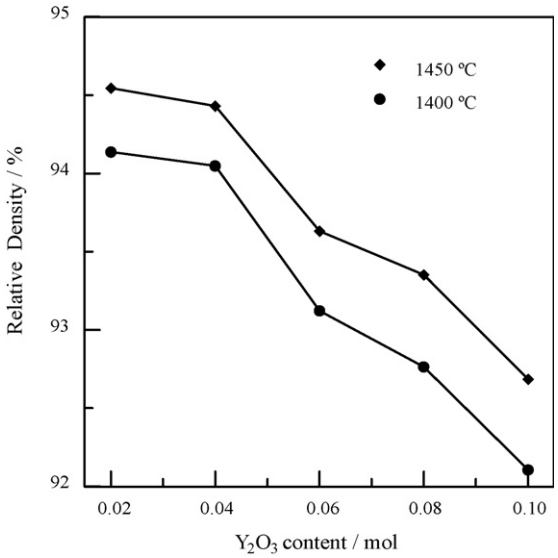

Fig. 4. Relative density of samples sintered at different temperatures.

3.4. Electrical conductivity and activation energy

Fig. 5 shows the relationship between log σ versus 1000/T of samples sintered at 1400 °C and 1450 °C in reducing atmosphere, respectively. The conductivity showed very good

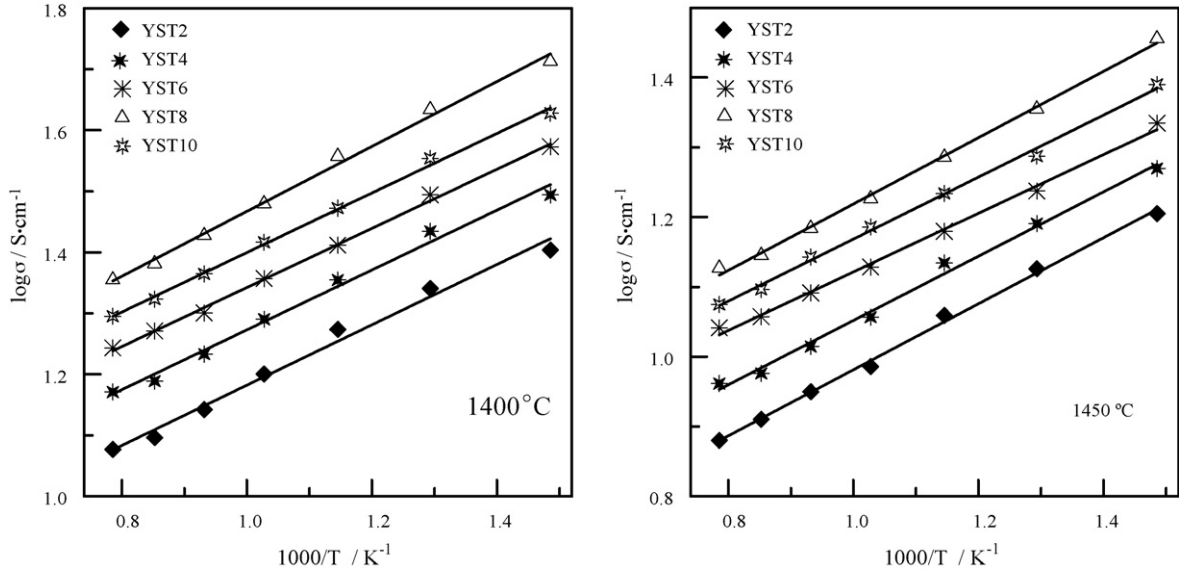

Fig. 5. Relationship between log σ vs. 1000/T for samples sintered at different temperatures.

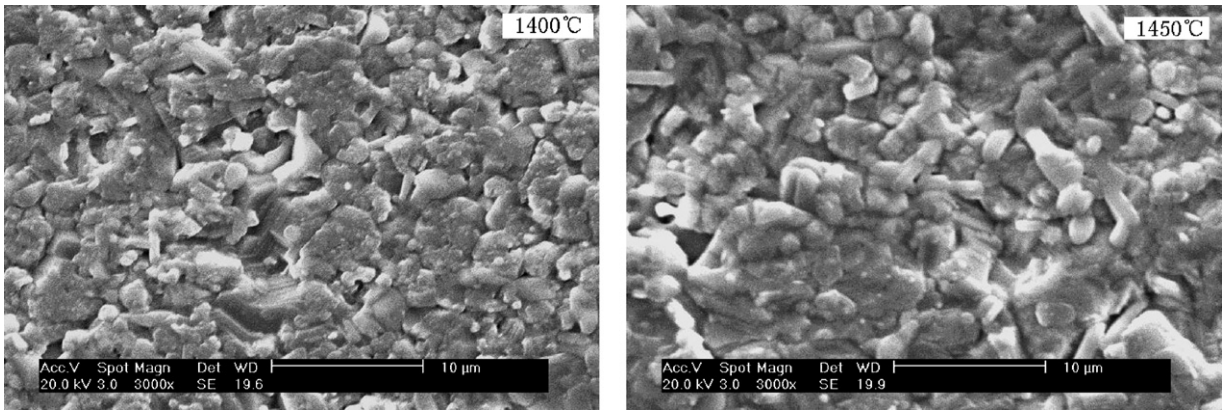

Fig. 6. SEM photographs of sample YST8 sintered at different temperatures.

reproducibility between heating and cooling after two or three cycles, when measured in reducing atmosphere. It can be seen that from 400 °C to 1000 °C, the conductivity decreased with increasing temperature. The high temperature and reducing atmosphere caused severe oxygen loss, forming high concentration of oxygen vacancies: $O_O \rightarrow (1/2)O_2 + V_O^{\bullet\bullet} + 2e'$, where O_O is oxygen ion, O_2 is one oxygen molecule, $V_O^{\bullet\bullet}$ is one oxygen vacancy, and e' is one free electron. Oxygen vacancies acted as scattering centers or trap-holes and the carrier mobility slowed down, which resulted in the conductivity decreasing with increasing temperature. The conductivity did not increase all the way with increasing Y_2O_3 content, but peaked at a certain content of Y_2O_3 dopant. Doping with Y_2O_3 in the crystal caused Sr vacancies and electrons. When excess Y_2O_3 was doped, the conductivity decreased as a result of the decrease in the number of charge carrier [14]. In addition, the formation of Sr vacancies presumably weakened the combination strength between oxygen ions and the surrounding Ti^{4+}; hence, oxygen would be easily released out of the crystal and oxygen vacancies would be formed when samples were heat-treated at high temperature in reducing atmosphere. The surrounding Ti^{4+} accepted one electron and transformed to Ti^{3+}, providing a charge carrying mechanism in these materials. Consequently, Y_2O_3-doped $SrTiO_3$ is believed to exhibit mixed electron-ion conductivity.

The conductivity of samples sintered at 1400 °C was higher than that of samples sintered at 1450 °C. The grain boundary resistance is a main factor with influence on the conduction of a semiconductor [15–17]. Although the high sintering temperature can facilitate grain growth, this may also cause the enhancement of grain boundary resistance with the increase in thickness of one insulating boundary layer, giving rise to a decrease in conductivity.

The $\log \sigma$ versus $1000/T$ plots for all samples showed almost a linearity, which illustrated that the relation between conductivity (σ) and temperature (T) follows the Arrhenius dependence: $\sigma = \sigma_0 \exp(-E_a/kT)$, where σ_0 is the pre-exponential factor; E_a the activation energy; k is the Boltzmann constant. The activation energy can be calculated from the slope of $\log \sigma = \log \sigma_0 - E_a/(2.303kT)$. The activation energy of samples lies between 0.095 eV and 0.111 eV. The activation energy of conductivity is an important parameter to evaluate the electrical conductivity of materials.

3.5. SEM observation

Fig. 6 shows the SEM photographs of Sample YST8 sintered at 1400 °C and 1450 °C, respectively. It can be clearly seen that the grain size of the sample sintered at 1400 °C was homogeneous. However, this material was not sufficiently densified at 1400 °C. With increasing sintering temperature to 1450 °C, grain growth proceeded and the material was sufficiently densified at this temperature. Additionally, some abnormal grain growth occurred in the sample sintered at 1450 °C. It is very likely that a thick grain boundary layer formed, causing a decrease in conductivity. This hypothesis is consistent with our results.

4. Conclusions

1. $SrTiO_3$ anode material doped with different Y_2O_3 contents was obtained by solid-state reaction. XRD analysis indicated that the yttrium-doped $SrTiO_3$ had a perovskite structure after calcination at 1100 °C for 2 h.
2. The conductivity of yttrium-doped $SrTiO_3$ is related to the sintering temperature and Y_2O_3 content. The highest conductivity at 800 °C (26.8 S/cm) of $Sr_{1-1.5x}Y_xTiO_3$ sintered at 1400 °C was observed for $x = 0.08$.
3. From 400 °C to 1000 °C, $Sr_{1-1.5x}Y_xTiO_3$ ($x = 0.02$, 0.04, 0.06, 0.08, 0.10) anode material possessed good conductance characteristics, which accord with Arrhenius formula. Conductivity decreased with increasing temperature.

References

[1] Z.F. Ma, W.M. Lin, Electrode materials study for solid oxide fuel cell. II: preparation and characterization of anode materials for methane oxidation, Chin. J. Power Sources 18 (1994) 10–12.
[2] W.Z. Zhu, S.C. Deevi, A review on the status of anode materials for solid oxide fuel cells, Mater. Sci. Eng. 362 (2003) 228–239.
[3] Y.X. Lu, S.A. Laura, Solid oxide fuel cell system fed with hydrogen sulfide and natural gas, J. Power Sources 135 (2004) 184–191.
[4] Sh.W. Tao, J.T.S. Irvine, Optimization of mixed conducting properties of Y_2O_3–ZrO_2–TiO_2 and Sc_2O_3–Y_2O_3–ZrO_2–TiO_2 solid solutions as potential SOFC anode materials, J. Solid State Chem. 165 (2002) 12–18.
[5] S.Zh. Wang, Y. Jiang, Electrochemical performance of mixed ionic–electronic conducting, Solid State Ionics 120 (1999) 75–84.

[6] R.J. Gorte, H. Kim, J.M. Vohs, Novel SOFC anodes for the direct electrochemical oxidation of hydrocarbon, J. Power Sources 106 (2002) 10–15.
[7] Z.J. Qu, Ch.Y. Yu, W.Zh. Li, The structure and labile oxygen of impurity-doped perovskite-type oxide, Acta Phys. Chim. Sin. 10 (1994) 796–801.
[8] J.W. Miao, Y.N. Fan, Y.Sh. Jin, A study of catalytic properties of doped $SrTiO_3$ catalysts for oxidative coupling of methane, Chem. Ind. Times 17 (2003) 21–24.
[9] Sh.Q. Hui, A. Petric, Electrical properties of yttrium-doped strontium titanate under reducing conditions, J. Electrochem. Soc. 149 (1) (2002) J1–J10.
[10] Sh.Q. Hui, A. Petric, Electrical conductivity of yttrium-doped $SrTiO_3$: influence of transition metal additives, Mater. Res. Bull. 37 (7) (2002) 1215–1231.
[11] P.D. Battle, J.E. Brnnett, J. Sloan, et al., A-site cation-vacancy ordering in $Sr_{1-3x/2}La_xTiO_3$: a study by HRTEM, J. Solid State Chem. 149 (2000) 360–369.
[12] R. Li, Q. Tang, S. Yin, et al., Sintering and characterization of $Ca_{0.9}Sr_{0.1}$-TiO_3 ceramics with sintering additive, Mater. Sci. Eng. A 373 (2004) 175–179.
[13] J.C.C. Abrantes, J.A. Labrincha, J.R. Frade, Behavior of strontium titanate ceramics in reducing conditions suggesting enhanced conductivity along grain contacts, J. Eur. Ceram. Soc. 22 (2002) 1683–1691.
[14] Y.H. Mo, R.B. Li, G.L. Zhou, Semiconductor Ceramics and Sensors, Shanghai Scientific and Technical Publishers, 1983, pp. 86–88.
[15] W.G. Menesklou, H.J. Schreiner, I.T. Ellen, High temperature oxygen sensors based on doped $SrTiO_3$, Sens. Actuators B 59 (1999) 184–189.
[16] S. Komornicki, J.C. Grenier, et al., Influence of stoichiometry on dielectric properties of boundary layer ceramics based on yttrium-doped strontium titanate, Mater. Sci. Eng. B: Solid-State Mater. Adv. Technol. 10 (2) (1991) 95–98.
[17] J.C.C. Abrantes, J.A. Labrincha, J.R. Frade, Applicability of the brick layer model to describe the grain boundary properties of strontium titanate ceramics, J. Eur. Ceram. Soc. 20 (2000) 1603–1609.